The Journal of General Physiology

Correction: S1–S3 counter charges in the voltage sensor module of a mammalian sodium channel regulate fast inactivation

James R. Groome and Vern Winston

Volume 141, No. 5, May 6, 2013. Pages 601–618.

In our 2013 paper in the Journal, we investigated the effects of mutations in the S1, S2, and S3 segments for each of the four domains of the voltage-gated sodium channel of skeletal muscle. As part of that work, we reported the effects of mutations on activation using I-V relations from experiments using the nonpermeant cation *N*-methyl-D-glucamine for internal and external recording solutions.

These conditions do not provide a measure of driving force as needed for a Boltzmann fit to obtain conductance parameters of midpoint and slope factor. Therefore, we have analyzed the original dataset using the asymptote for the relative change in current amplitude to estimate driving force and plot G-V relations. G/G_{MAX} was plotted as a function of voltage, and these curves were fit with a Boltzmann function to yield corrected values for midpoint and slope factor. These values and calculations for the change in free energy ($\Delta\Delta G^o$, $nzFV_{0.5}$) for mutations are provided in Table 3. Correction to plots for I-V relations given in the original paper are provided as extra panels for Figs. 2, 6, and 10. Fig. 11 has been replotted in its entirety. Table 3 and Figs. 2, 6, 10, and 11 are below.

The corrected parameters for activation of wild-type $hNa_V1.4$ in Table 3 are comparable to conductance measurements for the skeletal muscle sodium channel in other reports. Calculations of the change in free energy associated with activation of $hNa_V1.4$ yielded values of 2–3 kcal/mol for several mutations in the ENC and HCR of domains I–III, and the INC of domains I and II. These values are similar to those calculated for S1 and S2 countercharge mutations in NachBac (DeCaen et al., 2008, 2011). Our calculations of free energy differences are based on the effects of point mutations in a single domain of the skeletal muscle sodium channel, and interpretation of the role of S1–S3 countercharges based on those calculations should be limited.

In our original paper we concluded that negative countercharges in domains I–III are an important determinant of channel activation, most likely interacting with S4 positively charged residues to facilitate the outward movement of the voltage sensors in those domains in response to membrane depolarization. Further experimentation is needed to test our hypotheses about the general role of countercharge as a determinant of activation in $Na_V1.4$. In addition, we speculated that ENC and HCR countercharge residues in domains I and II may interact with outer positive charges in the S4 segments of these domains. A more recent study does show that ENC residues in domains I and II of $rNa_V1.4$ are important for channel activation (Pless et al., 2014). Future work describing the role of HCR or INC residues in activation is also needed to investigate the mechanisms by which S1–S3 countercharges affect sodium channel gating.

REFERENCES

DeCaen, P.G., V. Yarov-Yarovoy, Y. Zhao, T. Scheuer, and W.A. Catterall. 2008. Disulfide locking a sodium channel voltage sensor reveals ion pair formation during activation. *Proc. Natl. Acad. Sci. USA.* 105:15142–15147. http://dx.doi.org/10.1073/pnas.0806486105

DeCaen, P.G., V. Yarov-Yarovoy, T. Scheuer, and W.A. Catterall. 2011. Gating charge interactions with the S1 segment during activation of a Na^+ channel voltage sensor. *Proc. Natl. Acad. Sci. USA.* 108:18825–18830. http://dx.doi.org/10.1073/pnas.1116449108

Pless, S.A., F.D. Elstone, A.P. Niciforovic, J.D. Galpin, R. Yang, H.T. Kurata, and C.A. Ahern. 2014. Asymmetric functional contributions of acidic and aromatic side chains in sodium channel voltage-sensor domains. *J. Gen. Physiol.* 143:645–656. http://dx.doi.org/10.1085/jgp.201311036

TABLE 3

Equilibrium parameters for activation in wild-type and mutant sodium channels

Mutation	Location	$V_{0.5}$	Slope factor	$\Delta\Delta G^o$
		mV		*kcal/mol*
$hNa_v1.4$		−19.7 ± 1.4	5.28 ± 0.36	
ENC				
S151K	DI S1	−14.7 ± 1.5[a]	3.02 ± 0.13[b]	1.4
D152R	DI S1	−13.2 ± 1.0[c]	4.79 ± 0.14	0.9
E161R	DI S2	−8.93 ± 0.9[b]	4.92 ± 0.23	1.4
E598K	DII S1	9.76 ± 1.2[b]	3.46 ± 0.16[b]	3.2
N614K	DII S2	−1.56 ± 0.9[b]	3.83 ± 0.21[c]	2.3
E1051R	DIII S1	−7.01 ± 1.1[b]	4.11 ± 0.12[c]	1.7
E1051D	DIII S1	−9.85 ± 1.4[b]	4.11 ± 0.32[a]	1.5
D1069K	DIII S2	−2.11 ± 1.2[b]	3.67 ± 0.17[d]	2.2
D1069E	DIII S2	−17.4 ± 1.0	5.33 ± 0.35	0.3
E1373K	DIV S1	−17.7 ± 0.9	6.08 ± 0.32	−0.1
E1373N	DIV S1	−15.5 ± 1.2[a]	6.31 ± 0.53	0.1
E1373D	DIV S1	−17.4 ± 0.8	4.04 ± 0.14[c]	0.8
N1389K	DIV S2	−15.0 ± 1.2[a]	4.64 ± 0.22	0.8
N1389E	DIV S2	−18.5 ± 1.3	3.64 ± 0.20[d]	0.8
N1389D	DIV S2	−20.2 ± 1.2	4.57 ± 0.20	0.3
HCR				
N144K	DI S1	5.46 ± 1.8[b]	2.72 ± 0.19[b]	2.7
N144R	DI S1	−0.07 ± 1.4[b]	2.70 ± 0.19[b]	2.4
N144D	DI S1	−22.7 ± 0.7	3.72 ± 0.14[d]	0.5
N144E	DI S1	−19.1 ± 0.9	4.22 ± 0.20[a]	0.5
N591K	DII S1	−1.93 ± 1.3[b]	2.71 ± 0.17[b]	2.3
N591R	DII S1	0.96 ± 1.1[b]	2.56 ± 0.12[b]	2.5
N591D	DII S1	−0.11 ± 0.9[b]	3.45 ± 0.19[b]	2.4
N591E	DII S1	−18.4 ± 1.1	5.34 ± 0.29	0.1
S1044K	DIII S1	−13.7 ± 1.1[c]	4.06 ± 0.20[c]	1.1
S1044R	DIII S1	−4.12 ± 0.9[b]	3.19 ± 0.11[b]	2.1
S1044N	DIII S1	−15.1 ± 0.7[c]	4.44 ± 0.19[a]	0.9
S1044D	DIII S1	−19.0 ± 1.1	3.67 ± 0.28[c]	0.8
N1366K	DIV S1	−18.2 ± 1.8	4.88 ± 0.45	0.4
N1366R	DIV S1	−16.5 ± 1.3	5.42 ± 0.30	0.3
N1366D	DIV S1	−13.6 ± 1.2[c]	3.04 ± 0.19[b]	1.4
N1366E	DIV S1	−15.7 ± 1.2[a]	3.92 ± 0.20[c]	1.0
INC				
E171R	DI S2	−0.70 ± 1.6[b]	2.25 ± 0.09[b]	2.4
K175E	DI S2	−17.0 ± 0.9	4.45 ± 0.25	0.7
N194K	DI S3	−21.4 ± 1.2	4.03 ± 0.20[c]	0.4
D197R	DI S3	−3.22 ± 1.5[b]	2.54 ± 0.15[b]	2.2
E624K	DII S2	−8.88 ± 1.3[b]	3.67 ± 0.14[d]	1.6

TABLE 3 (*cont.*)

Mutation	Location	$V_{0.5}$	Slope factor	$\Delta\Delta G^o$
K628E	DII S2	−20.8 ± 0.7	4.66 ± 0.20	0.2
N643K	DII S3	−21.0 ± 0.6	4.97 ± 0.12	0.0
D646K	DII S3	−7.17 ± 1.3[b]	3.49 ± 0.21[d]	1.8
E1079R	DIII S2	−15.0 ± 1.0[c]	4.36 ± 0.37	0.9
K1083E	DIII S2	−16.9 ± 1.1	4.21 ± 0.22[a]	0.8
C1098K	DIII S3	−17.6 ± 1.3	3.59 ± 0.14[d]	0.9
D1101V	DIII S3	−16.9 ± 1.2	5.02 ± 0.46	0.4
E1399K	DIV S2	−17.2 ± 1.2	4.80 ± 0.23	0.5
K1403E	DIV S2	−16.4 ± 1.4	3.56 ± 0.24[d]	1.1
N1417K	DIV S3	−13.6 ± 0.9[d]	3.47 ± 0.17[b]	1.3
D1420K	DIV S3	−14.7 ± 1.3[a]	3.62 ± 0.18[d]	1.2

Midpoint voltage and slope factor for wild-type $hNa_V1.4$ and mutations of the extracellular charge region ENC, hydrophobic charge region HCR, and intracellular region INC, for segments S1–S3 in domains I–IV. Values represent mean ± SEM and were obtained from the Boltzmann fits to plots of G/G_{MAX} shown in Figs. 2 (ENC), 6 (HCR), and 10 (INC). $\Delta\Delta G^o$ values were calculated as $nzFV_{0.5}$ from mean midpoint voltage.

[a]$P \leq 0.05$.

[b]$P \leq 0.0001$.

[c]$P \leq 0.01$.

[d]$P \leq 0.001$.

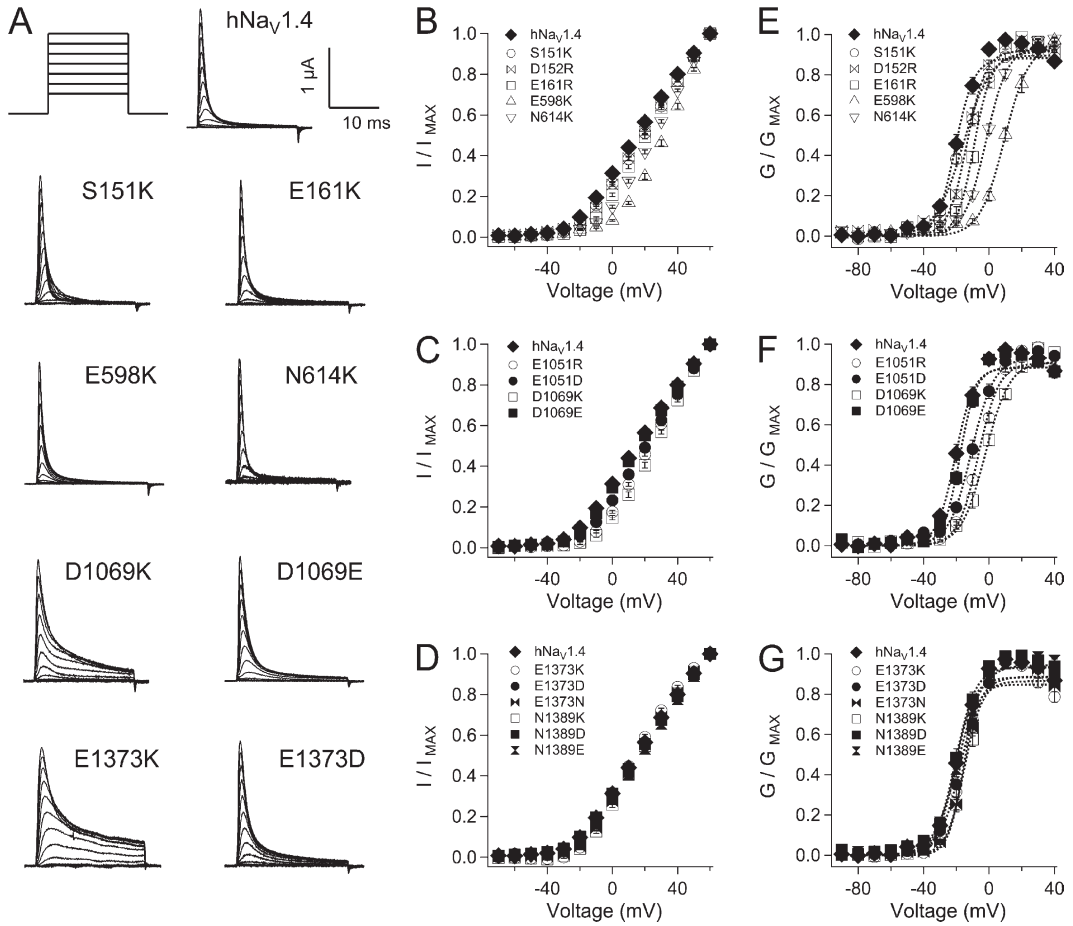

Figure 2. Conductance in $hNa_V1.4$ and ENC mutations. (A) Traces for wild-type and mutant channels in response to depolarizing commands to voltages ranging from −90 to 60 mV. I-V relations are shown for ENC mutations in domains I and II (B), domain III (C), and domain IV (D). Values represent mean ± SEM (error bars) from 10–22 experiments. Additional panels are shown for g-V relations in domains I and II (E), domain III (F), and domain IV (G). Boltzmann fits to each plot are shown by dotted lines.

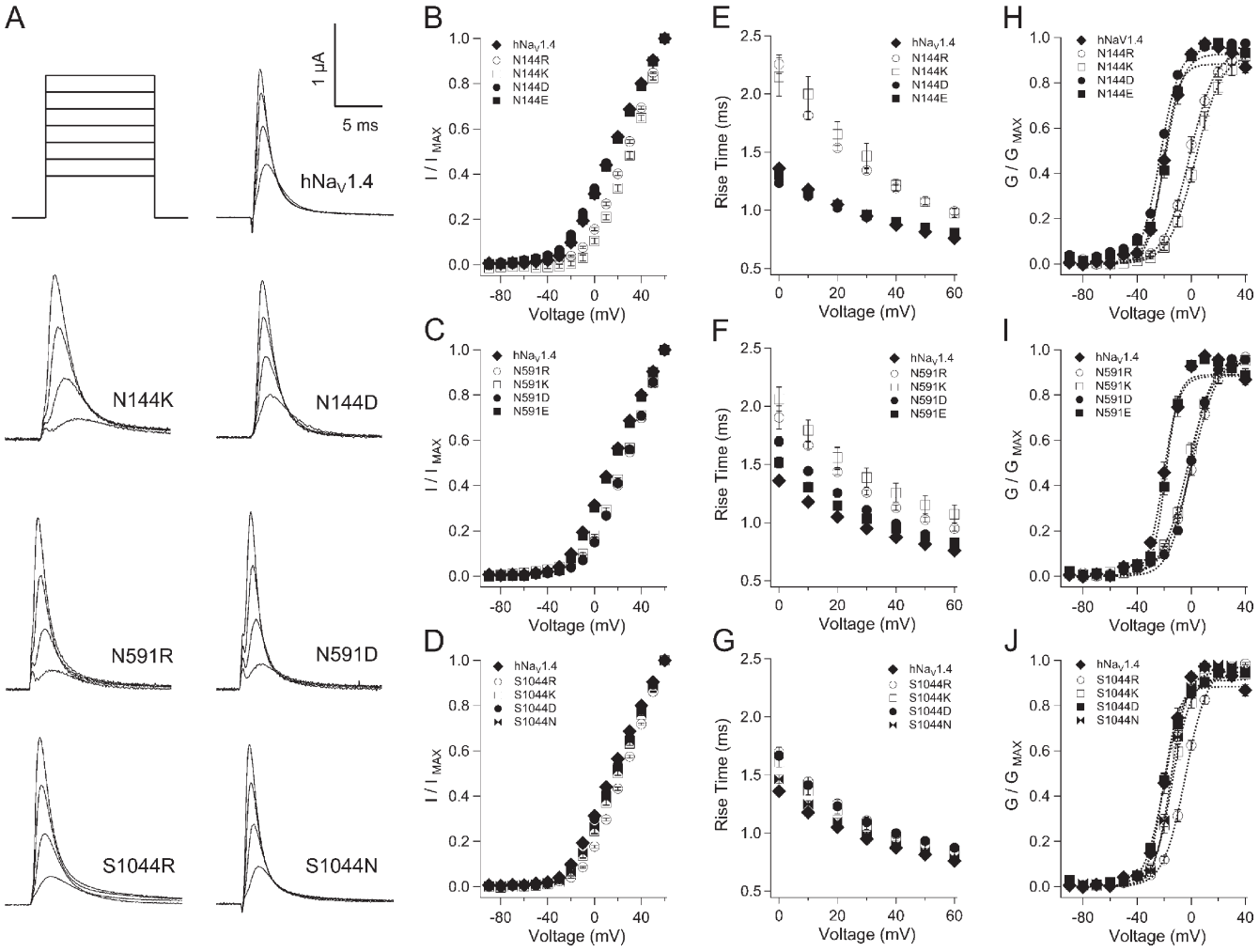

Figure 6. Activation parameters for mutations at S1 HCR locus in $hNa_V1.4$. (A) Traces shown are responses to depolarization to 0, 20, 40, and 60 mV for mutations in domains I–III. Plots in B, D, and F show I-V relations for mutations in these domains; plots in C, E, and G show activation kinetics. Values represent mean ± SEM (error bars) from 11–24 experiments. Additional panels are shown for g-V relations for $hNa_V1.4$ and mutations of the HCR in domain I (H), domain II (I), and domain III (J). Boltzmann fits to each plot are shown by dotted lines.

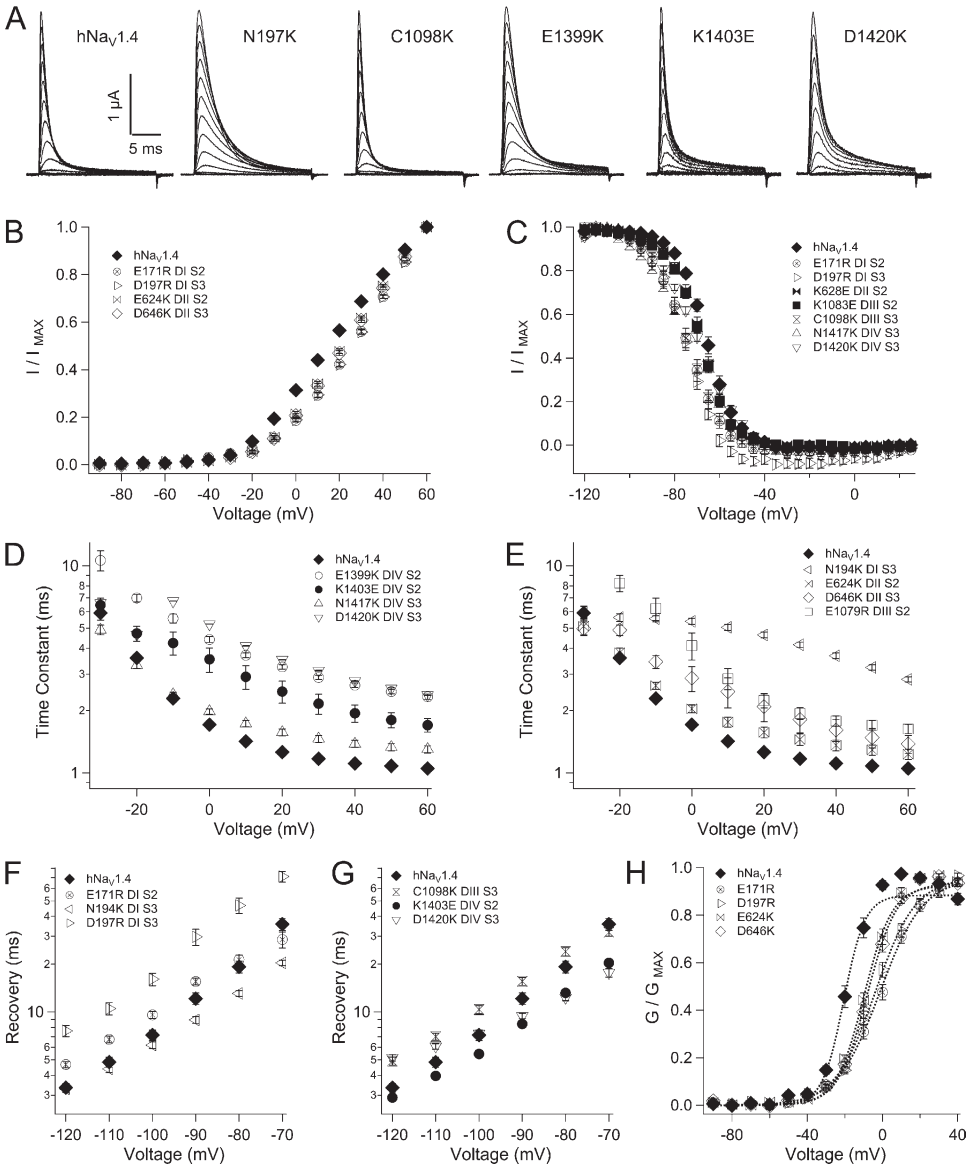

Figure 10. Biophysical characterization of INC mutations. (A) Sodium currents in response to command depolarization to voltages from −90 to 60 mV. Effects of INC mutations are shown for activation (B), steady-state fast inactivation (C), entry into fast inactivation (D and E), and recovery (F and G). Legends identify residues and locus by domain and segment. Values represent mean ± SEM (error bars) from 10–23 experiments. The additional panel (H) is shown for g-V relations for $hNa_V1.4$ and mutations of the INC in domains I and II. Boltzmann fits to each plot are shown by dotted lines.

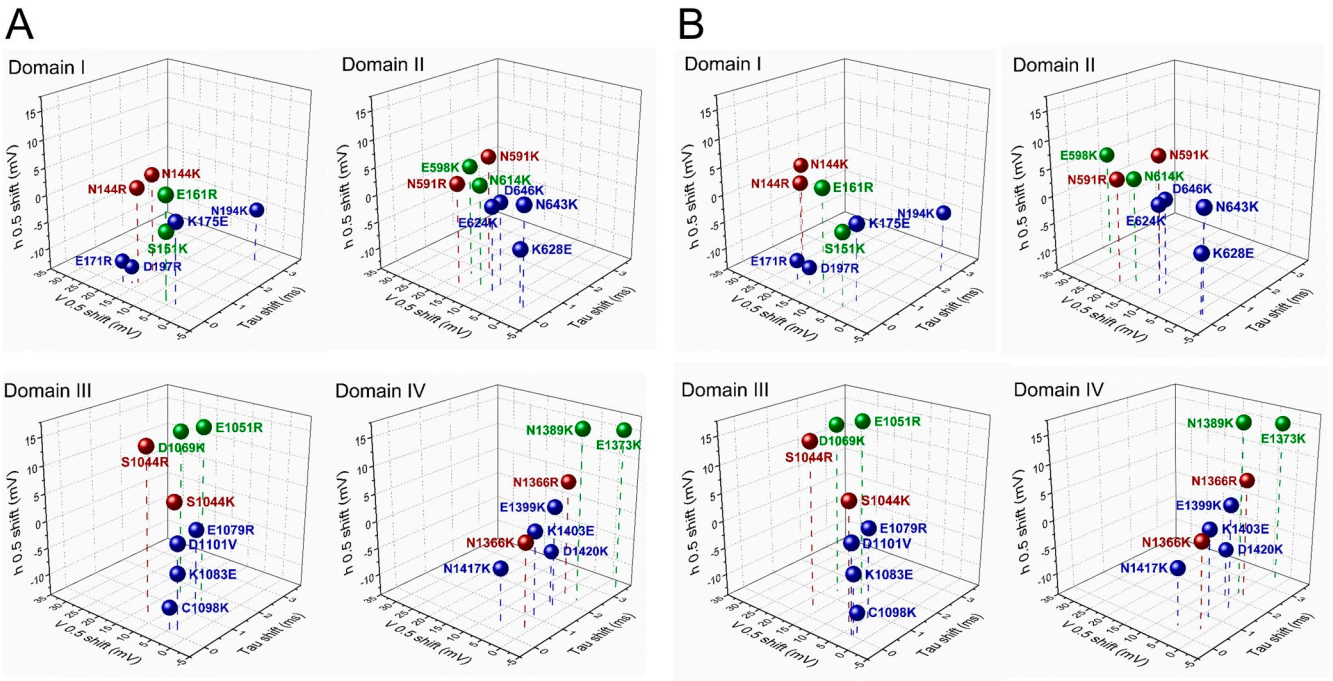

Figure 11. Three-dimensional plot showing the effect of charge-reversing mutations of residues in ENC (green), HCR (red), and INC (blue) regions. Shown for each domain are shifts in inactivation kinetics at 20 mV (x axis), activation probability (y axis), and inactivation probability (z axis). Corrected values for $V_{0.5}$ shifts shown in B are calculated from g-V relations of Table 3.